Origin of Negative Longitudinal Piezoelectric Effect

Shi Liu[1,*] and R. E. Cohen[1,2,†]
[1]Extreme Materials Initiative, Geophysical Laboratory, Carnegie Institution for Science, Washington, DC 20015-1305, USA
[2]Department of Earth- and Environmental Sciences, Ludwig Maximilians Universität, Munich 80333, Germany
(Received 23 August 2017; published 14 November 2017)

Piezoelectrics with negative longitudinal piezoelectric coefficients will contract in the direction of an applied electric field. Such piezoelectrics are thought to be rare, but there is no fundamental physics preventing the realization of negative longitudinal piezoelectric effect in a single-phase material. Using first-principles calculations, we demonstrate that several hexagonal *ABC* ferroelectrics possess significant negative longitudinal piezoelectric effects. The data mining of a first-principles-based database of piezoelectrics reveals that this effect is a general phenomenon. The origin of this unusual piezoelectric response relies on the strong ionic bonds associated with small effective charges and rigid potential energy surfaces. Moreover, ferroelectrics with negative longitudinal piezoelectric coefficients show anomalous pressure-enhanced ferroelectricity. Our results offer design principles to aid the search for new piezoelectrics for novel electromechanical device applications.

DOI: 10.1103/PhysRevLett.119.207601

Piezoelectrics are a class of functional materials that can convert electrical energy to mechanical energy and vice versa. They serve as critical components in many modern devices ranging from medical ultrasound, fuel injectors, and sonar, to vibration-powered electronics [1]. Piezoelectricity is usually gauged by the piezoelectric coefficient that characterizes how the polarization changes in response to a stress or strain. This leads to two piezoelectric equations: one links the induced polarization in direction α (ΔP_α) with an applied stress with component j (σ_j , stress in Voigt notion) described by $\Delta P_\alpha = d_{\alpha j}\sigma_j$, where $d_{\alpha j}$ is the piezoelectric strain coefficient; another one connects ΔP_α with strain (η) given by $\Delta P_\alpha = e_{\alpha j}\eta_j$, where $e_{\alpha j}$ is the piezoelectric stress coefficient [2,3]. Both $d_{\alpha j}$ and $e_{\alpha j}$ are third-rank tensors, and they are related to each other via elastic compliances $d_{\alpha j} = S_{jk}e_{\alpha k}$.

Piezoelectricity is a bulk effect [4] and contains a clamped-ion contribution evaluated at vanishing microscopic strain and an internal-strain contribution due to the relative displacement of atoms in response to the macroscopic strain [5,6]. The "improper" piezoelectric tensor defined as $\partial P_\alpha/\partial\eta_j$ includes the contributions to the linear order due to polarization rotation or dilation [6,7]. The modern theory of polarization [8–11] shows that polarization is only well defined modulo a polarization quantum and takes on a lattice of values (P^b, where b is a "branch" label). The "proper" piezoelectric coefficient that measures the adiabatic change of the current density resulting from a slow crystal deformation is well defined and does not suffer from any branch dependence. It is the proper piezoelectric coefficient that should be compared to experiments where piezoelectric coefficients are measured based on the charge flow through the sample [12]. In this Letter, we focus on proper piezoelectric coefficients unless explicitly stated otherwise.

The longitudinal piezoelectric coefficients (e_{33} and d_{33}, assuming the polar axis is in the z direction) are almost always positive: consequently, a tensile strain (uniaxial stretching) increases the polarization, or equivalently, the lattice expands along the direction of an applied electric field, as one would expect from the displacements of charged ions in electric fields. One well-known exception is the ferroelectric polymer poly(vinylidene fluoride) (PVDF) and its copolymers which possess a *negative* longitudinal piezoelectric effect (NLPE): the polymers will contract in the direction of an applied electric field [13–15]. The NLPE in PVDF is attributed to the unique microstructures of PVDF polymers with intermixed crystalline lamellae and amorphous regions [15]. Though counterintuitive, the NLPE has received very little attention. In fact, no measurements of NLPE for single-phase materials have been reported in the literature. Previous first-principles studies reported that several III-V zinc-blende compounds (e.g., GaAs and GaSb) have small negative e_{33} (≈ -0.1 C/m^2, where the threefold axis of the cubic zinc-blende unit cell is assumed as the z direction) [16]; wurtzite BN has a relatively large (more negative) $e_{33} = -0.94$ C/m^2 [17,18]. However, the origin of NLPE in single-phase materials is not clear.

We first consider the piezoelectric properties of a family of *ABC* ferroelectrics recently discovered through first-principles high-throughput density functional theory (DFT) computations [19]. As a variant of the half-Heusler structure, hexagonal *ABC* ferroelectrics are in the polar space group $P6_3mc$, same as that of wurtzite BN, and the unit cell has six atoms with *B* and *C* atoms forming buckling honeycomb layers separated by layers of *A* atoms. Several *ABC* ferroelectrics (e.g., LiBeSb) are found to possess so-called "hyperferroelectricity" characterized by the persistent polarization even at the zero displacement field boundary condition [20–22]. It was suggested that short-range

repulsions is likely to play an important role in driving the ferroelectric instability in the paraelectric $P6_3/mcm$ phase [23].

Our DFT calculations reveal that a few *ABC* ferroelectrics possess significant NLPE. Among all studied *ABC* ferroelectrics, KMgSb has the most negative d_{33} of -19 pC/N, whereas LiMgAs has the most positive d_{33} of 29 pC/N; both compare well to known piezoelectrics such as ZnO with $d_{33} \approx 20$ pC/N [24–26]. By screening through a database of calculated intrinsic piezoelectric constants for 941 inorganic crystalline compounds [27], we find that NLPE is a general phenomenon; more than 90 compounds have negative e_{33} and 52 of the compounds were already reported in the Inorganic Crystal Structural Database (ICSD). Moreover, we find that the electric polarization of several *ABC* ferroelectrics increases in magnitude as a hydrostatic pressure is applied, making them appealing for high-pressure applications.

All first-principles calculations are carried out using ABINIT [28,29] with local density approximation and an $8 \times 8 \times 8$ Monkhorst-Pack sampling for the hexagonal lattice. We used ultrasoft pseudopotentials from the Garrity, Bennett, Rabe, Vanderbilt high-throughput pseudopotential set [30] and a plane-wave cutoff of 25 Ha and a charge density cutoff of 125 Ha. A force convergence threshold of 1.0×10^{-5} Ha/bohr and Gaussian smearing of 1 mHa are used to fully relax the lattice constants and atomic positions. The hexagonal crystal, with the c axis in the z direction, has three independent piezoelectric coefficients, e_{15}, e_{31}, and e_{33}. We focus on the longitudinal piezoelectric coefficients e_{33} and d_{33}, which are evaluated with density functional perturbation theory (DFPT) [31] and a larger plane-wave cutoff of 30 Ha and charge density cutoff of 250 Ha. The electromechanical coupling factor $k_{\alpha j}$, an important figure of merit for piezoelectrics that measures the effectiveness of energy conversion, can be estimated with $k_{33} = |d_{33}|/\sqrt{\varepsilon_{33} S_{33}}$, where ε is the zero-stress dielectric tensor, and S is the compliance tensor [32].

We first study 14 *ABC* semiconducting ferroelectrics [19] with DFPT and calculate the piezoelectric constants, compliances, stress-free dielectric constants, and electromechanical coupling factors reported in Table I. The values of $|e_{33}|$ range from 0.37 to 1.54 C/m^2, and $|d_{33}|$ range from 2.25 to 28.6 pC/N compared well with many III-V nitrides such as AlN, GaN, and InN ($e_{33} \approx 1.0$–1.5 C/m^2 and $d_{33} \approx 2$–8 pC/N) [16,18,33]. Notably, the piezoelectric properties of LiMgP ($e_{33} = 1.5$ C/m^2, $d_{33} = 25$ pC/N, $k_{33} = 0.45$) compare favorably with classic piezoelectric ZnO ($e_{33} = 0.96$ C/m^2, $d_{33} = 12.3$ pC/N, $k_{33} = 0.41$) [32] and potentially can serve as a new lead-free high-performance piezoelectric made of earth-abundant elements. Moreover, a few *ABC* ferroelectrics exhibit NLPE characterized by negative e_{33} and d_{33}: NaZnSb has the most negative e_{33} of -1.04 C/m^2 and KMgSb has the most negative d_{33} of -19 pC/N.

TABLE I. Theoretical values of piezoelectric coefficients e_{33} (C/m^2) and d_{33} (pC/N), compliance $S_{33}(10^{-11}\ \mathrm{Pa}^{-1})$, zero-stress dielectric constant ε_{33}, and electromechanical coupling coefficient k_{33} for *ABC* ferroelectrics. Materials with negative e_{33} are underscored.

ABC	e_{33}	d_{33}	S_{33}	ε_{33}	k_{33}
LiBeP	−0.49	−3.42	0.58	16.6	0.117
LiMgP	1.51	24.66	1.64	20.6	0.451
LiZnP	0.57	3.44	0.70	24.3	0.088
LiBeAs	−0.48	−3.70	0.65	17.6	0.117
LiMgAs	1.54	28.60	1.88	23.2	0.461
LiZnAs	0.37	2.25	0.81	28.0	0.050
LiBeSb	−0.66	−5.31	0.74	19.0	0.150
LiZnSb	−0.56	−5.76	0.92	30.6	0.115
LiBeBi	−0.76	−7.26	0.89	23.0	0.171
NaMgP	0.58	7.80	1.83	20.6	0.135
NaMgAs	0.57	8.44	1.96	21.5	0.138
NaMgSb	0.49	8.09	2.06	20.8	0.131
NaZnSb	−1.04	−17.30	1.43	25.0	0.308
KMgSb	−0.42	−19.15	3.14	19.6	0.259

To understand the origin of NLPE, we decompose e_{33} into two terms [6],

$$e_{33} = \bar{e}_{33} + e'_{33}, \tag{1}$$

where $\bar{e}_{33}$ is the clamped-ion term computed with the internal atomic coordinates (u) fixed at their zero-strain values and

$$e'_{33} = \sum_s \frac{ec}{\Omega} Z^*_{33} \frac{\partial u_3(s)}{\partial \eta_3} \tag{2}$$

is the internal-strain term arising from the internal microscopic atomic relaxations in response to a macroscopic strain η_3 applied in the z direction. Here, s runs over the atoms in the unit cell of volume Ω, e is the electron charge, c is the lattice constant along the polar axis of the hexagonal unit cell, and Z^*_{33} is the Born effective charge associated with the displacement of u_3. We find that for *ABC* ferroelectrics with NLPE, the negative clamped-ion $\bar{e}_{33}$ dominates the total response, whereas the internal-strain contribution e'_{33}, though being positive for most compounds, is not large enough to compensate the negative $\bar{e}_{33}$ (Table II). From Eq. (2), the value of e'_{33} depends on the values of effective charges and the coupling of internal coordinates with the macroscopic strain [34]. One can see that the Born effective charges of *ABC* ferroelectrics (Table II) are close to the nominal ionic charges, in sharp contrast with typical ferroelectric perovskites such as $PbTiO_3$, where the Born effective charges are much larger than the formal charges. This suggests that the ferroelectricity in hexagonal *ABC* is most likely driven by the geometric ionic size effects [35–38] rather than the chemical bonding effect such as the p-d orbital hybridization in transition metal oxides [39]. Moreover, the response of internal coordinates to the

TABLE II. Born effective charges Z^*_{33}, clamped-ion $\bar{e}_{33}$ (C/m^2), internal-strain e'_{33} (C/m^2), total e_{33} (C/m^2) for *ABC* ferroelectrics. Materials with negative e_{33} are underscored.

ABC	$Z^*_{33}(A)$	$Z^*_{33}(B)$	$Z^*_{33}(C)$	$[\partial u_3(B)/\partial\eta_3]$	$[\partial u_3(C)/\partial\eta_3]$	$\bar{e}_{33}$	e'_{33}	e_{33}
LiBeP	1.18	1.04	−2.22	−0.11	−0.07	−0.63	0.14	−0.49
LiMgP	0.93	1.85	−2.77	−0.19	−0.40	−0.11	1.62	1.51
LiZnP	1.22	1.58	−2.80	−0.11	−0.22	−0.62	1.19	0.57
LiBeAs	1.21	0.99	−2.20	−0.09	−0.07	−0.65	0.17	−0.48
LiMgAs	0.94	1.84	−2.78	−0.21	−0.43	−0.12	1.66	1.54
LiZnAs	1.29	1.66	−2.95	−0.13	−0.24	−0.73	1.10	0.37
LiBeSb	1.30	0.55	−1.85	0.02	−0.01	−0.70	0.04	−0.66
LiZnSb	1.43	1.39	−2.82	0.06	−0.04	−0.95	0.39	−0.56
LiBeBi	1.35	0.61	−1.96	0.04	0.01	−0.76	0.01	−0.76
NaMgP	0.99	1.92	−2.90	−0.08	−0.19	−0.24	0.81	0.58
NaMgAs	1.01	1.90	−2.91	−0.09	−0.21	−0.26	0.83	0.57
NaMgSb	1.10	1.85	−2.95	−0.04	−0.19	−0.32	0.82	0.49
NaZnSb	1.06	1.76	−2.81	−0.04	−0.01	−0.95	−0.09	−1.04
KMgSb	0.70	2.01	−2.71	−0.10	−0.05	−0.39	−0.03	−0.42
$PbTiO_3$	3.53	5.51	−4.61	0.22	−0.31	−0.86	6.06	5.20

macroscopic strain characterized by $\partial u_3(s)/\partial\eta_3$ is also substantially smaller and negative than those in $PbTiO_3$ [e.g., $\partial u_3(\mathrm{Pb})/\partial\eta_3 = 0.36$ and $\partial u_3(\mathrm{Ti})/\partial\eta_3 = 0.22$]. Taking LiBeSb as an example, the total response $e_{33} = -0.66$ C/m^2 is mainly associated with $\bar{e}_{33} = -0.7$ C/m^2, and the small e'_{33} is due to the small effective charges, $Z^*_{33}(\mathrm{Be}) = 0.55\ e$ and $Z^*_{33}(\mathrm{Sb}) = -1.85\ e$, and nearly zero $\partial u_3(s)/\partial\eta_3$. We also note that for *ABC* ferroelectrics with positive e_{33}, the piezoelectric response is mainly due to the displacement of *C* atoms, as reflected by the relatively large $Z^*_{33}(C)$ and $\partial u_3(C)/\partial\eta_3$.

Our first-principles calculations indicate that the NLPE occurs when the negative clamped-ion piezoelectric response dominates over the internal-strain contribution. It is, therefore, more likely to realize NLPE in piezoelectrics with strong ionic bonds, which may be associated with small effective charges and small atomic relaxations in response to a macroscopic strain. Using a database of piezoelectrics recently developed via high-throughput DFT calculations [27], we search for materials with negative e_{33} through a large pool of compounds (941 inorganic compounds). We focus on materials with $|e_{33}|$ being the largest tensor element and $e_{33} < -0.1$ C/m^2. Much to our surprise, we find 93 compounds with negative e_{33}, among which 52 compounds are documented in ICSD (see the Supplemental Material [40]). Notable examples are $AgNO_3$ (ICSD code 374, $R3c$, $e_{33} = -0.60$ C/m^2), VPO_3 (ICSD code 152278, $P4mm$, $e_{33} = -2.05$ C/m^2), and KIO_3 (ICSD code 97995, $R3m$, $e_{33} = -1.36$ C/m^2).

One feature of ferroelectrics with NLPE is the increase of electrical polarization with the decrease of lattice constant along the polar axis, which hints toward the presence of unusual pressure dependence of ferroelectricity. As hydrostatic pressure generally reduces the lattice constants, ferroelectrics with NLPE may have the polarization enhanced at high pressure. This is different from conventional ferroelectrics, in which the polarization will decrease and eventually vanish with increasing hydrostatic pressure [41–44].

We calculate the electrical polarization as a function of hydrostatic pressure for 13 *ABC* ferroelectrics that remain insulating between 0 and 10 GPa (Fig 1). As expected, LiBeP, LiBeAs, LiBeSb, LiZnSb, LiBeBi, and KMgSb, all possessing NLPE, have enhanced polarization with the increasing pressure. There are two exceptions: LiZnP and LiZnAs have positive e_{33} but also show pressure-enhanced ferroelectricity. This can be understood by $\Delta P_3 = 2e^{\mathrm{IP}}_{31}\eta_1 + e^{\mathrm{IP}}_{33}\eta_3$, where e^{IP}_{31} and e^{IP}_{33} are the improper piezoelectric constants, and η_1 ($\eta_1 = \eta_2$) and η_3 are pressure-induced

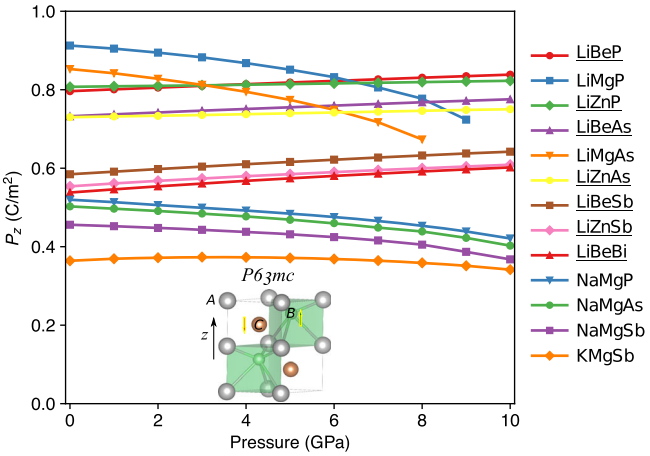

FIG. 1. Polarization along the *c* axis (P_z) of *ABC* ferroelectrics as a function of hydrostatic pressure. Materials exhibiting pressure-enhanced ferroelectricity are underscored. The electrical polarization of KMgSb increases with the pressure until 3 GPa. The inset shows the structure of hexagonal *ABC* ferroelectrics.

strains. Here, the improper piezoelectric coefficients are used because they include the pure volume effect on the polarization. The proper to improper piezoelectric coefficients are related by the spontaneous polarization, $e_{31}^{\mathrm{IP}} = e_{31} - P_3$ and $e_{33}^{\mathrm{IP}} = e_{33}$ [12]. Therefore, the pressure-enhanced polarization in LiZnP and LiZnAs is due to the negative $e_{31}^{\mathrm{IP}} = -0.47\ \mathrm{C/m^2}$ for LiZnP and $e_{31}^{\mathrm{IP}} = -0.38\ \mathrm{C/m^2}$ for LiZnAs. We note that similar pressure-enhanced ferroelectricity is reported for improper ferroelectrics such as hexagonal $R\mathrm{FeO_3}$ (R = Ce, Gd, Lu), where a zone-boundary phonon mode associated with the tilt of $\mathrm{FeO_5}$ bipyramid is responsible for the anomalous pressure dependence [45]. However, *ABC* ferroelectrics are proper ferroelectrics, and the zone-center Γ_2^- mode is the primary order parameter responsible for the transition from paraelectric $P6_3/mmc$ phase to polar $P6_3mc$ phase.

Further investigations of *ABC* ferroelectrics at higher pressures up to 85 GPa reveal that the ferroelectric polarization can be extremely robust. Taking LiBeSb as an example, we find that the polarization keeps increasing with increasing pressure [Fig. 2(a)]. Meanwhile, the band gap becomes smaller and eventually closes at 75 GPa. Electronic band structure and phonon spectrum (calculated with phonopy code [46]) confirm that LiBeSb at 85 GPa is a stable semimetal with bands across the Fermi energy, though the structure remains in the polar space group $P6_3mc$ [Figs. 2(b) and 2(c)]. This is surprising because the long-range electrostatic dipole-dipole interaction that favors the break of inversion symmetry should be screened out by the free electrons in metal. The observation that LiBeSb at 85 GPa is a noncentrosymmetric semimetal further suggests that the ferroelectricity is likely due to the geometric effect which is not coupled with states near the Fermi level.

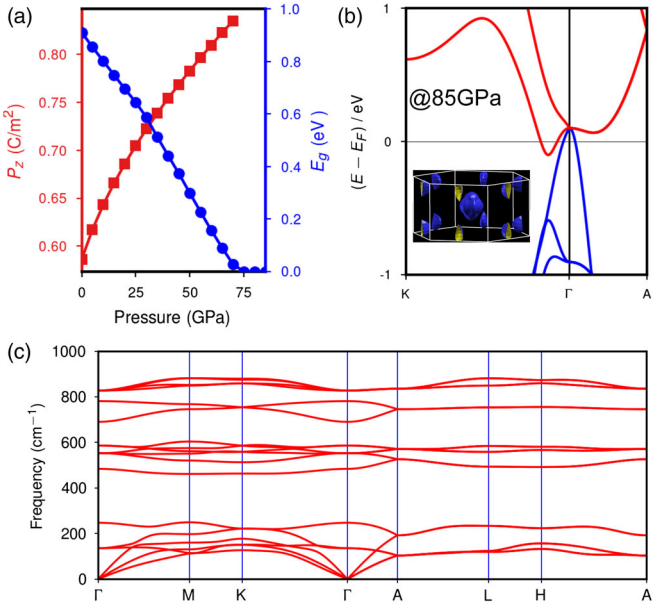

FIG. 2. (a) Ferroelectric polarization and band gap of LiBeSb as a function of hydrostatic pressure. (b) Electronic band structure and (c) phonon spectrum of LiBeSb in the polar space group $P6_3mc$ at 85 GPa. The inset shows the Fermi surface near the Γ point.

In summary, we have explained the origin of negative longitudinal piezoelectric effect with first-principles density functional theory calculations. This counterintuitive piezoelectric response turns out to be a general phenomenon arising from the negative clamped-ion piezoelectric response. The data mining of a database of piezoelectrics leads to more than 90 compounds possessing negative e_{33}. The electrical polarization of *ABC* ferroelectrics is robust against pressure, and the pressure-enhanced ferroelectricity is intimately related to their unusual piezoelectric properties. We hope that this work will inspire future experimental studies of negative longitudinal piezoelectric effect, which may offer novel avenues for designing nanoscale electromechanical devices.

This work is partly supported by U.S. Office of Naval Research Grants No. N00014-12-1-1038 and No. N00014-14-1-0561. S. L. and R. E. C. are supported by the Carnegie Institution for Science. R. E. C. is also supported by the European Research Council Advanced Grant ToMCaT. Computational support was provided by the U.S. DOD from the HPCMO.

*sliu@carnegiescience.edu
†rcohen@carnegiescience.edu

[1] Y. Mao, P. Zhao, G. McConohy, H. Yang, Y. Tong, and X. Wang, Adv. Energy Mater. **4**, 1301624 (2014).
[2] J. F. Nye, *Physical Properties of Crystals: Their Representation by Tensors and Matrices* (Oxford University Press, New York, 1985).
[3] L. Bellaiche, Curr. Opin. Solid State Mater. Sci. **6**, 19 (2002).
[4] R. M. Martin, Phys. Rev. B **5**, 1607 (1972).
[5] S. de Gironcoli, S. Baroni, and R. Resta, Phys. Rev. Lett. **62**, 2853 (1989).
[6] G. Sághi-Szabó, R. E. Cohen, and H. Krakauer, Phys. Rev. Lett. **80**, 4321 (1998).
[7] D. F. Nelson and M. Lax, Phys. Rev. B **13**, 1785 (1976).
[8] R. D. King-Smith and D. Vanderbilt, Phys. Rev. B **47**, 1651 (1993).
[9] R. D. King-Smith and D. Vanderbilt, Phys. Rev. B **49**, 5828 (1994).
[10] R. Resta, Europhys. Lett. **22**, 133 (1993).
[11] R. Resta, Rev. Mod. Phys. **66**, 899 (1994).
[12] D. Vanderbilt, J. Phys. Chem. Solids **61**, 147 (2000).
[13] T. Furukawa, J. X. Wen, K. Suzuki, Y. Takashina, and M. Date, J. Appl. Phys. **56**, 829 (1984).
[14] V. S. Bystrov, E. V. Paramonova, I. K. Bdikin, A. V. Bystrova, R. C. Pullar, and A. L. Kholkin, J. Mol. Model. **19**, 3591 (2013).
[15] I. Katsouras, K. Asadi, M. Li, T. B. van Driel, K. S. Kjær, D. Zhao, T. Lenz, Y. Gu, P. W. M. Blom, D. Damjanovic,

M. M. Nielsen, and D. M. de Leeuw, Nat. Mater. **15**, 78 (2015).
[16] F. Bernardini, V. Fiorentini, and D. Vanderbilt, Phys. Rev. B **56**, R10024 (1997).
[17] K. Shimada, T. Sota, K. Suzuki, and H. Okumura, Jpn. J. Appl. Phys. **37**, L1421 (1998).
[18] K. Shimada, Jpn. J. Appl. Phys. **45**, L358 (2006).
[19] J. W. Bennett, K. F. Garrity, K. M. Rabe, and D. Vanderbilt, Phys. Rev. Lett. **109**, 167602 (2012).
[20] K. F. Garrity, K. M. Rabe, and D. Vanderbilt, Phys. Rev. Lett. **112**, 127601 (2014).
[21] H. Fu, J. Appl. Phys. **116**, 164104 (2014).
[22] S. Liu and R. E. Cohen, J. Phys. Condens. Matter **29**, 244003 (2017).
[23] P. Li, X. Ren, G.-C. Guo, and L. He, Sci. Rep. **6**, 34085 (2016).
[24] M. Catti, Y. Noel, and R. Dovesi, J. Phys. Chem. Solids **64**, 2183 (2003).
[25] *Low Frequency Properties of Dielectric Crystals: Piezoelectronic, Pyroelectric and Related Constants*, edited by O. Madelun (Springer, Berlin, 1993), Vol. 29b.
[26] V. Coleman and C. Jagadish, *Zinc Oxide Bulk, Thin Films and Nanostructures* (Elsevier, New York, 2006), pp. 1–20.
[27] M. de Jong, W. Chen, H. Geerlings, M. Asta, and K. A. Persson, Sci. Data **2**, 150053 (2015).
[28] X. Gonze, J.-M. Beuken, R. Caracas, F. Detraux, M. Fuchs, G.-M. Rignanese, L. Sindic, M. Verstraete, G. Zerah, F. Jollet, M. Torrent, A. Roy, M. Mikami, P. Ghosez, J.-Y. Raty, and D. Allan, Comput. Mater. Sci. **25**, 478 (2002).
[29] X. Gonze *et al.*, Comput. Phys. Commun. **180**, 2582 (2009).
[30] K. F. Garrity, J. W. Bennett, K. M. Rabe, and D. Vanderbilt, Comput. Mater. Sci. **81**, 446 (2014).
[31] X. Gonze and C. Lee, Phys. Rev. B **55**, 10355 (1997).
[32] X. Wu, D. Vanderbilt, and D. R. Hamann, Phys. Rev. B **72**, 035105 (2005).
[33] F. Bernardini and V. Fiorentini, Appl. Phys. Lett. **80**, 4145 (2002).
[34] J. Íñiguez, D. Vanderbilt, and L. Bellaiche, Phys. Rev. B **67**, 224107 (2003).
[35] B. B. V. Aken, T. T. Palstra, A. Filippetti, and N. A. Spaldin, Nat. Mater. **3**, 164 (2004).
[36] C. Ederer and N. A. Spaldin, Nat. Mater. **3**, 849 (2004).
[37] T. Tohei, H. Moriwake, H. Murata, A. Kuwabara, R. Hashimoto, T. Yamamoto, and I. Tanaka, Phys. Rev. B **79**, 144125 (2009).
[38] A. C. Garcia-Castro, N. A. Spaldin, A. H. Romero, and E. Bousquet, Phys. Rev. B **89**, 104107 (2014).
[39] R. E. Cohen, Nature (London) **358**, 136 (1992).
[40] See Supplemental Material at http://link.aps.org/supplemental/10.1103/PhysRevLett.119.207601 for the results of the data mining of a first-principles-based database of piezoelectrics.
[41] G. A. Samara, Ferroelectrics **2**, 277 (1971).
[42] G. A. Samara, T. Sakudo, and K. Yoshimitsu, Phys. Rev. Lett. **35**, 1767 (1975).
[43] I. A. Kornev, L. Bellaiche, P. Bouvier, P.-E. Janolin, B. Dkhil, and J. Kreisel, Phys. Rev. Lett. **95**, 196804 (2005).
[44] Z. Wu and R. E. Cohen, Phys. Rev. Lett. **95**, 037601 (2005).
[45] C. Xu, Y. Yang, S. Wang, W. Duan, B. Gu, and L. Bellaiche, Phys. Rev. B **89**, 205122 (2014).
[46] A. Togo and I. Tanaka, Scr. Mater. **108**, 1 (2015).